

Synthesis, Crystal Structure, and Solid-State NMR Spectroscopy of a New Open-Framework Aluminophosphate $(\text{NH}_4)_2\text{Al}_4(\text{PO}_4)_4(\text{HPO}_4)\cdot\text{H}_2\text{O}$

Dan Zhou,[†] Lei Chen,[‡] Jihong Yu,^{*,†} Yi Li,[†] Wenfu Yan,[†] Feng Deng,^{*,‡} and Ruren Xu[†]

State Key Laboratory of Inorganic Synthesis and Preparative Chemistry, College of Chemistry, Jilin University, Changchun 130012, People's Republic of China, and State Key Laboratory of Magnetic Resonance and Atomic and Molecular Physics, Wuhan Institute of Physics and Mathematics, The Chinese Academy of Sciences, Wuhan 430071, People's Republic of China

Received November 1, 2004

A new three-dimensional open-framework aluminophosphate $(\text{NH}_4)_2\text{Al}_4(\text{PO}_4)_4(\text{HPO}_4)\cdot\text{H}_2\text{O}$ (denoted AIPO-CJ19) with an Al/P ratio of 4/5 has been synthesized, using pyridine as the solvent and 2-aminopyridine as the structure-directing agent, under solvothermal conditions. The structure was determined by single-crystal X-ray diffraction and further characterized by solid-state NMR techniques. The alternation of the Al-centered polyhedra (including AlO_4 , AlO_5 , and AlO_6) and the P-centered tetrahedra (including PO_4 and PO_3OH) results in an interrupted open-framework structure with an eight-membered ring channel along the [100] direction. This is the first aluminophosphate containing three kinds of Al coordinations (AlO_4 , AlO_5 , and AlO_6) with all oxygen vertexes connected to framework P atoms. ^{27}Al MAS NMR, ^{31}P MAS NMR, and $^1\text{H} \rightarrow ^{31}\text{P}$ CPMAS NMR characterizations show that the solid-state NMR techniques are an effective complement to XRD analysis for structure elucidation. Furthermore, all of the possible coordinations of Al and P in the aluminophosphates with an Al/P ratio of 4/5 are summarized. Crystal data: $(\text{NH}_4)_2\text{Al}_4(\text{PO}_4)_4(\text{HPO}_4)\cdot\text{H}_2\text{O}$, monoclinic $P2_1$ (No. 4), $a = 5.0568(3)$ Å, $b = 21.6211(18)$ Å, $c = 8.1724(4)$ Å, $\beta = 91.361(4)^\circ$, $V = 893.27(10)$ Å³, $Z = 2$, $R_1 = 0.0456$ ($I > 2\sigma(I)$), and $wR_2 = 0.1051$ (all data).

Introduction

Since the discovery of aluminophosphate $\text{AIPO}_4\text{-}n$ (n denotes a specific structure type) molecular sieves in the early 1980s,¹ a large number of new microporous aluminophosphate materials have been successfully synthesized under hydrothermal or solvothermal conditions.^{2–7} In contrast to neutral-framework $\text{AIPO}_4\text{-}n$, composed of strictly alternating AlO_4 and PO_4 tetrahedra connected through corner-sharing

vertex oxygen atoms with an Al/P ratio of exclusively unity, a variety of aluminophosphates with anionic chains, layers, and open frameworks with an Al/P ratio of less than unity have been synthesized.⁸ These anionic aluminophosphates are constructed from the alternation of Al polyhedra (AlO_4 , AlO_5 , and AlO_6) and P tetrahedra (PO_{4b} , PO_{3b}O_t , $\text{PO}_{2b}\text{O}_{2t}$, and PO_bO_{3t} where b represents bridging oxygens and t represents terminal oxygens), and their Al/P ratios are 1/2, 2/3, 3/4, 3/5, 4/5, 5/6, 11/12, 12/13, and 13/18.

Organic amines play an important role in the formation of microporous materials by acting as a template or structure-directing agent.⁹ Different organic amines can direct the same structure, and one organic amine can lead to different kinds of inorganic structures. An open-framework aluminophosphate, AIPO-CJ4, containing propeller-like chiral motifs with an Al/P ratio of 1/2, produced using 2-aminopyridine as the structure-directing agent and butan-2-ol as the solvent, has been reported.¹⁰ In this work, a new three-dimensionally

* To whom correspondence should be addressed. E-mail: jihong@mail.jlu.edu.cn. Fax: +86-431-5168608. Tel.: +86-431-5168608.

[†] Jilin University.

[‡] The Chinese Academy of Sciences.

- (1) Wilson, S. T.; Lok, B. M. C.; Messina, A.; Cannan, T. R.; Flanigen, E. M. *J. Am. Chem. Soc.* **1982**, *104*, 1146.
- (2) Bennett, J. M.; Richardson, J. W., Jr.; Pluth, J. J.; Smith, J. V. *Zeolites* **1987**, *7*, 160.
- (3) Davis, M. E.; Saldarriaga, C.; Montes, C.; Garces, J.; Crowder, C. *Nature* **1988**, *331*, 698.
- (4) Wei, B.; Zhu, G.; Yu, J.; Qiu, S.; Xiao, F.; Terasaki, O. *Chem. Mater.* **1999**, *11*, 3417.
- (5) Yan, W.; Yu, J.; Xu, R.; Zhu, G.; Xiao, F.; Han, Y.; Sugiyama, K.; Terasaki, O. *Chem. Mater.* **2000**, *12*, 2517.
- (6) Wang, K.; Yu, J.; Miao, P.; Song, Y.; Li, J.; Shi, Z.; Xu, R. *J. Mater. Chem.* **2001**, *11*, 1898.
- (7) Rao, C. N. R.; Natarajan, S.; Choudhury, A.; Neeraj, S.; Ayi, A. A. *Acc. Chem. Res.* **2001**, *34*, 80.

(8) Yu, J.; Xu, R. *Acc. Chem. Res.* **2003**, *36*, 481.

(9) Lok, B. M.; Cannan, T. R.; Messina, C. A. *Zeolites* **1983**, *3*, 282 and references therein.

(10) Yan, W.; Yu, J.; Shi, Z.; Xu, R. *Chem. Commun.* **2000**, 1431.

connected open-framework aluminophosphate with an Al/P ratio of 4/5 (AIPO-CJ19) has been synthesized successfully in the $\text{Al}(\text{OPr}^i)_3\text{-H}_3\text{PO}_4\text{-2-aminopyridine-pyridine}$ system. Since the discovery of AIPO-HDA,¹¹ Mu-4,¹² and SIZ-1,¹³ AIPO-CJ19 is the fourth type of anionic framework aluminophosphate with an Al/P ratio of 4/5. AIPO-CJ19 has a network of strictly alternating Al units, including AlO_4 , AlO_5 , AlO_6 , and P tetrahedra, including PO_{4b} and PO_{3b}OH .

Solid-state NMR spectroscopy has been proven to be an efficient tool for structural elucidation and chemical analysis in aluminophosphates and related materials.^{14–17} In this work, solid-state NMR techniques have been employed to characterize the coordination of the Al and P atoms of AIPO-CJ19. The results are in good agreement with the structure determined by the single-crystal XRD analysis. The coordinations of the Al and P atoms of the aluminophosphates were found to determine the Al/P ratio.⁸ Various possible coordinations of Al and P which can result in an Al/P ratio of 4/5 are summarized.

Experimental Section

Synthesis and Characterization. AIPO-CJ19 was synthesized in the $\text{Al}(\text{OPr}^i)_3\text{-H}_3\text{PO}_4\text{-2-aminopyridine-pyridine}$ reaction system with an optimized molar composition range of 1.0/2.0–4.0/2.0–6.0/23. Typically, 1.0 g of finely ground aluminum triisopropoxide was dispersed into 9 mL of pyridine solvent with stirring, followed by addition of 2.76 g of 2-aminopyridine. Phosphoric acid (1.33 mL, 85 wt % in water) was added dropwise to the above reaction mixture with stirring. The reaction mixture was stirred until it was homogeneous, and then it was sealed in a Teflon-lined stainless autoclave and heated under autogenous pressure at 180 °C for 8 days. The resulting product, containing colorless platelike single crystals, was separated using sonication, washed with deionized water, and dried at room temperature. The yield of the product was about 70% based on the source of $\text{Al}(\text{OPr}^i)_3$.

The type of solvent was important for the crystallization of AIPO-CJ19. When butan-2-ol was used as the solvent instead of pyridine, the product was AIPO-CJ4,¹⁰ whereas when other solvents were used with the other conditions unchanged, no crystalline product could be produced. On the other hand, 2-aminopyridine was also important for the synthesis of AIPO-CJ19. Even though it was not occluded in the final product, 2-aminopyridine might play a structure-directing role in the formation of AIPO-CJ19.⁹ This phenomenon is commonly observed in the synthesis of zeolite and zeolite-like materials, such as $\text{AlPO}_4\text{-15}$ ¹⁸ and AIPO-CJ4.¹⁰ In the absence of 2-aminopyridine, AIPO-CJ19 could not be obtained.

Table 1. Crystal Data and Structure Refinement for AIPO-CJ19^a

empirical formula	$\text{H}_{11}\text{Al}_4\text{N}_2\text{O}_{21}\text{P}_5$
fw	637.88
temp	293(2) K
wavelength	0.71073 Å
cryst syst, space group	monoclinic, $P2_1$
unit cell dimensions	$a = 5.0568(3)$ Å $b = 21.6211(18)$ Å $c = 8.1724(4)$ Å $\beta = 91.361(4)^\circ$
vol	$893.27(10)$ Å ³
Z, calcd density	2, 2.372 Mg/m ³
abs coeff	0.827 mm^{-1}
$F(000)$	640
cryst size	$0.40 \times 0.10 \times 0.05\text{ mm}^3$
θ for data collection	$2.67\text{--}24.97^\circ$
limiting indices	$-6 \leq h \leq 5, -14 \leq k \leq 25, -9 \leq l \leq 9$
reflns collected/unique	4664/2046 [$R(\text{int}) = 0.0655$]
completeness to $\theta = 24.97$	96.4%
refinement method	full-matrix least-squares on F^2
data/restraints/parameters	2046/13/289
GOF on F^2	0.782
final R indices [$I > 2\sigma(I)$] ^a	$R_1 = 0.0456, wR_2 = 0.1051$
R indices (all data)	$R_1 = 0.0702, wR_2 = 0.1219$
largest diff. peak and hole	1.493 and -0.562 e \AA^{-3}

^a $R_1 = \sum(\Delta F/\sum(F_o))$, $R_2 = (\sum[w(F_o^2 - F_c^2)])/\sum[w(F_o^2)^{1/2}]$, and $w = 1/\sigma^2(F_o^2)$.

X-ray powder diffraction (XRD) data were collected in the 2θ range of $4\text{--}40^\circ$ on a Siemens D5005 diffractometer with $\text{Cu K}\alpha$ radiation ($\lambda = 1.5418$ Å). The step size was 0.01° , and the step time was 12 s. Inductively coupled plasma (ICP) analysis was performed on a Perkin-Elmer Optima 3300Dv spectrometer. Elemental analyses were conducted on a Perkin-Elmer 2400 elemental analyzer. Thermogravimetric analysis (TGA) was carried out on a Perkin-Elmer TGA 7 unit in air with a heating rate of $20^\circ\text{C}/\text{min}$.

Structure Determination. A suitable single crystal with dimensions of $0.40 \times 0.10 \times 0.5\text{ mm}^3$ was selected for single-crystal X-ray diffraction analysis. Structural analysis was performed on a Siemens SMART CCD diffractometer using graphite-monochromated $\text{Mo K}\alpha$ radiation ($\lambda = 0.71073$ Å) at a temperature of $20 \pm 2^\circ\text{C}$. Data processing was accomplished with the SAINT processing program.¹⁹ Direct methods were used to solve the structure using the SHELXL crystallographic software package.²⁰ Two possible space groups were suggested: one is centrosymmetric $P2_1/c$, and the other is noncentrosymmetric $P2_1$. The structure could not be properly solved using the $P2_1/c$ space group. Therefore, the $P2_1$ space group was selected for the structural solution. All framework Al, P, and O atoms could be unambiguously located. The three atoms subsequently located from the difference Fourier map were suggested to be associated with one H_2O and two protonated NH_3 molecules by charge balance and elemental analysis. The H atom in P-OH group was added geometrically and refined in a riding model. The non-hydrogen atoms were refined anisotropically. Structure details and selected bond lengths and distances are listed in Tables 1 and 2, respectively.

Solid-State NMR Measurements. The solid-state ^{31}P NMR experiments were carried out at a resonance frequency of 161.97 MHz on a Varian Infinityplus-400 spectrometer using a Chemagnetic 5 mm triple-resonance probe. The ^{31}P single-pulse experiment was performed with a $2.0\text{ }\mu\text{s}$ pulse width ($\pi/4$) and a 180 s recycle delay. A $^1\text{H} \rightarrow ^{31}\text{P}$ cross-polarization magic-angle spinning

- (11) Yu, J.; Sugiyama, K.; Zheng, S.; Qiu, S.; Chen, J.; Xu, R.; Sakamoto, Y.; Terasaki, O.; Hiraga, K.; Light, M.; Hursthouse, M. B.; Thomas, J. M. *Chem. Mater.* **1998**, *10*, 1208.
- (12) Vidal, L.; Gramlich, V.; Patarin, J.; Gabelica, Z. *Eur. J. Solid State Inorg. Chem.* **1998**, *35*, 545.
- (13) Cooper, E. R.; Andrews, C. D.; Wheatley, P. S.; Webb, P. B.; Wormald, P.; Morris, R. E. *Nature* **2004**, *430*, 1012.
- (14) Taulelle, F.; Pruski, M.; Amoureux, J. P.; Lang, D.; Bailly, A.; Huguenard, C.; Haouas, M.; Gérardin, C.; Loiseau, T.; Férey, G. J. *Am. Chem. Soc.* **1999**, *121*, 12148.
- (15) Luo, Q.; Deng, F.; Yuan, Z.; Yang, J.; Zhang, M.; Yue, Y.; Ye, C. J. *Phys. Chem. B* **2003**, *107*, 2435.
- (16) Loiseau, T.; Férey, G.; Haouas, M.; Taulelle, F. *Chem. Mater.* **2004**, *16*, 5318.
- (17) Huang, Y. N.; Richer, R.; Kirby, C. W. *J. Phys. Chem. B* **2003**, *107*, 1326.
- (18) Pluth, J. J.; Smith, J. V.; Bennet, J. M.; Cohen, J. P. *Acta Crystallogr., Sect. C* **1984**, *40*, 2008.

(19) SMART and SAINT; Siemens Analytical X-ray Instruments, Inc.: Madison, WI, 1996.

(20) Sheldrick, G. M. SHELXL, version 5.1; Siemens Industrial Automation, Inc.: Madison, WI, 1997.

Table 2. Bond Lengths (Å) and Angles (deg) for AIPO-CJ19^a

Al(1)–O(6)	1.738(8)	Al(1)–O(1)	1.741(8)
Al(1)–O(14)#1	1.755(9)	Al(1)–O(4)#2	1.764(8)
Al(2)–O(18)	1.742(7)	Al(2)–O(11)#3	1.787(8)
Al(2)–O(12)	1.826(8)	Al(2)–O(7)#4	1.873(9)
Al(2)–O(13)	1.932(10)	Al(3)–O(8)	1.825(8)
Al(3)–O(5)	1.835(9)	Al(3)–O(3)	1.897(10)
Al(3)–O(10)#5	1.900(10)	Al(3)–O(19)	1.926(8)
Al(3)–O(17)	1.995(7)	Al(4)–O(9)	1.709(9)
Al(4)–O(2)	1.728(8)	Al(4)–O(15)#2	1.729(9)
Al(4)–O(16)	1.785(9)	P(1)–O(3)	1.503(10)
P(1)–O(2)	1.527(8)	P(1)–O(4)	1.537(8)
P(1)–O(1)	1.546(8)	P(2)–O(8)#2	1.494(8)
P(2)–O(5)	1.517(9)	P(2)–O(7)	1.548(8)
P(2)–O(6)	1.549(9)	P(3)–O(10)	1.500(9)
P(3)–O(11)	1.519(8)	P(3)–O(12)	1.532(8)
P(3)–O(9)	1.568(9)	P(4)–O(13)	1.495(10)
P(4)–O(16)	1.496(9)	P(4)–O(14)	1.525(8)
P(4)–O(15)	1.549(8)	P(5)–O(17)	1.506(7)
P(5)–O(19)#3	1.506(7)	P(5)–O(18)#6	1.533(7)
P(5)–O(20)	1.615(10)		
O(6)–Al(1)–O(1)	112.1(4)	O(6)–Al(1)–O(14)#1	110.5(4)
O(1)–Al(1)–O(14)#1	107.8(4)	O(6)–Al(1)–O(4)#2	112.8(5)
O(1)–Al(1)–O(4)#2	107.9(4)	O(14)#1–Al(1)–O(4)#2	105.5(4)
O(18)–Al(2)–O(11)#3	134.4(5)	O(18)–Al(2)–O(12)	119.5(4)
O(11)#3–Al(2)–O(12)	105.8(4)	O(18)–Al(2)–O(7)#4	88.5(4)
O(11)#3–Al(2)–O(7)#4	92.5(4)	O(12)–Al(2)–O(7)#4	94.8(4)
O(18)–Al(2)–O(13)	85.7(4)	O(11)#3–Al(2)–O(13)	88.5(4)
O(12)–Al(2)–O(13)	92.0(4)	O(7)#4–Al(2)–O(13)	172.7(4)
O(8)–Al(3)–O(5)	97.1(4)	O(8)–Al(3)–O(3)	91.5(4)
O(5)–Al(3)–O(3)	92.4(4)	O(8)–Al(3)–O(10)#5	88.2(4)
O(5)–Al(3)–O(10)#5	92.7(4)	O(3)–Al(3)–O(10)#5	174.8(4)
O(8)–Al(3)–O(19)	168.2(4)	O(5)–Al(3)–O(19)	94.7(4)
O(3)–Al(3)–O(19)	87.9(4)	O(10)#5–Al(3)–O(19)	91.3(4)
O(8)–Al(3)–O(17)	84.6(4)	O(5)–Al(3)–O(17)	177.9(4)
O(3)–Al(3)–O(17)	86.3(3)	O(10)#5–Al(3)–O(17)	88.5(4)
O(19)–Al(3)–O(17)	83.6(3)	O(9)–Al(4)–O(2)	110.8(4)
O(9)–Al(4)–O(15)#2	110.7(4)	O(2)–Al(4)–O(15)#2	105.1(4)
O(9)–Al(4)–O(16)	110.4(4)	O(2)–Al(4)–O(16)	110.8(5)
O(15)#2–Al(4)–O(16)	109.0(4)	O(3)–P(1)–O(2)	108.0(5)
O(3)–P(1)–O(4)	111.4(5)	O(2)–P(1)–O(4)	108.7(5)
O(3)–P(1)–O(1)	114.6(5)	O(2)–P(1)–O(1)	107.6(4)
O(4)–P(1)–O(1)	106.3(4)	O(8)#2–P(2)–O(5)	113.4(5)
O(8)#2–P(2)–O(7)	109.9(5)	O(5)–P(2)–O(7)	112.0(5)
O(8)#2–P(2)–O(6)	109.7(5)	O(5)–P(2)–O(6)	107.7(5)
O(7)–P(2)–O(6)	103.7(5)	O(10)–P(3)–O(11)	114.7(6)
O(10)–P(3)–O(12)	108.8(5)	O(11)–P(3)–O(12)	109.2(5)
O(10)–P(3)–O(9)	106.9(5)	O(11)–P(3)–O(9)	108.4(5)
O(12)–P(3)–O(9)	108.8(5)	O(13)–P(4)–O(16)	112.3(5)
O(13)–P(4)–O(14)	106.6(5)	O(16)–P(4)–O(14)	108.8(5)
O(13)–P(4)–O(15)	110.2(5)	O(16)–P(4)–O(15)	109.4(5)
O(14)–P(4)–O(15)	109.5(5)	O(17)–P(5)–O(19)#3	115.3(4)
O(17)–P(5)–O(18)#6	111.3(4)	O(19)#3–P(5)–O(18)#6	108.6(4)
O(17)–P(5)–O(20)	109.6(5)	O(19)#3–P(5)–O(20)	109.8(4)
O(18)#6–P(5)–O(20)	101.3(5)	P(1)–O(1)–Al(1)	145.4(5)
P(1)–O(2)–Al(4)	148.9(6)	P(1)–O(3)–Al(3)	146.2(5)
P(1)–O(4)–Al(1)#3	133.8(6)	P(2)–O(5)–Al(3)	140.5(5)
P(2)–O(6)–Al(1)	131.6(5)	P(2)–O(7)–Al(2)#5	132.0(5)
P(2)#3–O(8)–Al(3)	155.5(7)	P(3)–O(9)–Al(4)	136.0(5)
P(3)–O(10)–Al(3)#4	136.6(6)	P(3)–O(11)–Al(2)#2	142.5(7)
P(3)–O(12)–Al(2)	139.4(5)	P(4)–O(13)–Al(2)	149.4(5)
P(4)–O(14)–Al(1)#7	142.4(6)	P(4)–O(15)–Al(4)#3	131.8(6)
P(4)–O(16)–Al(4)	145.5(6)	P(5)–O(17)–Al(3)	128.7(4)
P(5)#8–O(18)–Al(2)	141.9(5)	P(5)#2–O(19)–Al(3)	147.5(5)
P(5)–O(20)–H(1)	109.5		

^a Symmetry transformations used to generate equivalent atoms are as follows: #1 $x + 1, y, z + 1$; #2 $x + 1, y, z$; #3 $x - 1, y, z$; #4 $-x + 3, y + 1/2, -z + 3$; #5 $-x + 3, y - 1/2, -z + 3$; #6 $-x + 2, y - 1/2, -z + 2$; #7 $x - 1, y, z - 1$.

(CPMAS) NMR spectrum was recorded using conventional Hartmann–Hahn cross-polarization with a ¹H $\pi/2$ pulse duration of 4.6 μ s, a contact time of 0.2 ms, and a recycle delay of 5.0 s. ¹H decoupling with a field strength of 40 kHz was applied during the acquisition period. ²⁷Al MAS NMR spectra were obtained at two

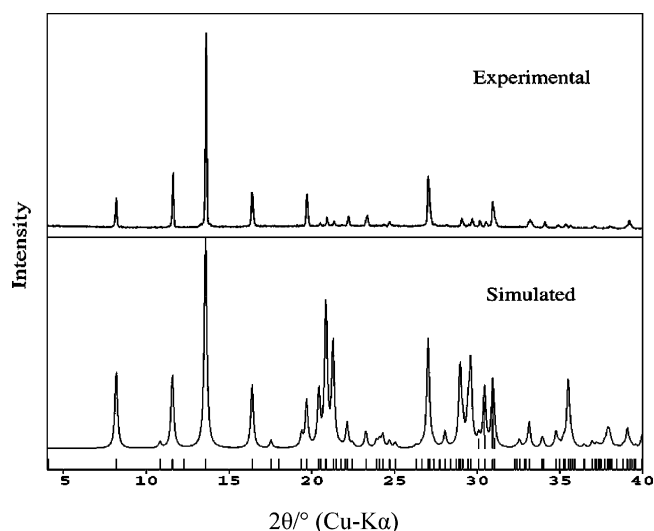


Figure 1. Experimental and simulated X-ray diffraction patterns of AIPO-CJ19.

different fields, 7.1 (78.12 MHz) and 9.4 T (104.26 MHz), on Varian Infinityplus spectrometers. Typical acquisition conditions were the following: a single-pulse excitation, a short pulse width of 0.5 μ s (corresponding to a $\pi/15$ flip angle), and a recycling delay of 1.0 s. The MAS spin rate was 8 kHz in single-pulse and CP experiments. The chemical shifts were referenced to a 0.1 M Al(NO₃)₃ solution for ²⁷Al and to an 85% H₃PO₄ solution for ³¹P.

Results and Discussion

The experimental and simulated powder X-ray diffraction (XRD) patterns of AIPO-CJ19 are shown in Figure 1. They are in good agreement with each other which proves the phase purity of the as-synthesized product. The difference in reflection intensity is probably due to the preferred orientation effect in the powder sample.²¹ The absence of some reflections might be a result of their relatively low intensity.

ICP analysis gives the contents of Al and P as 16.7 and 24.4 wt %, respectively (calcd: Al, 16.92; P, 24.28 wt %). Elemental analysis gives the contents of H and N as 1.70 and 4.42 wt %, respectively (calcd: H, 1.74; N, 4.39 wt %). No carbon element is detected, indicating that no template molecule is involved in the product. The compositional analysis results are in agreement with the empirical formula, (NH₄)₂Al₄(PO₄)₄(HPO₄)·H₂O, given by single-crystal structure analysis.

The TG curve in Figure 2 shows the two stages of weight loss occurring at 150–700 °C. The first weight loss, a total of 7.54 wt % at 150–360 °C, corresponds to the loss of the H₂O and NH₃ molecules (calcd 8.16 wt %). The second loss of 2.48 wt % at 360–700 °C corresponds to the loss of the –OH moiety attached to P in the form of H₂O (calcd 2.82 wt %).²² Powder XRD analysis indicates that AIPO-CJ19 becomes amorphous upon calcination at 300 °C for 4 h.

(21) Wang, K.; Yu, J.; Miao, P.; Song, Y.; Li, J.; Shi, Z.; Xu, R. *J. Mater. Chem.* **2001**, *11*, 1898.

(22) Yuan, H. M.; Chen, J. S.; Shi, Z.; Chen, W.; Wang, Y.; Zhang, P.; Yu, J.; Xu, R. *J. Chem. Soc., Dalton Trans.* **2000**, 1981.

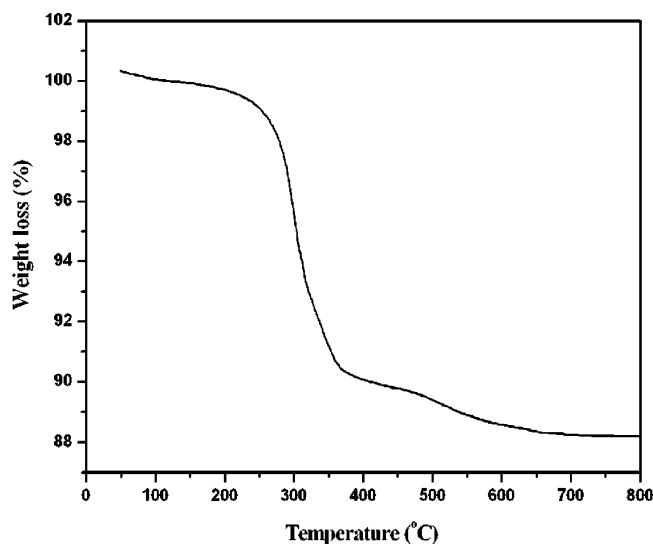


Figure 2. TG curve of AIPO-CJ19.

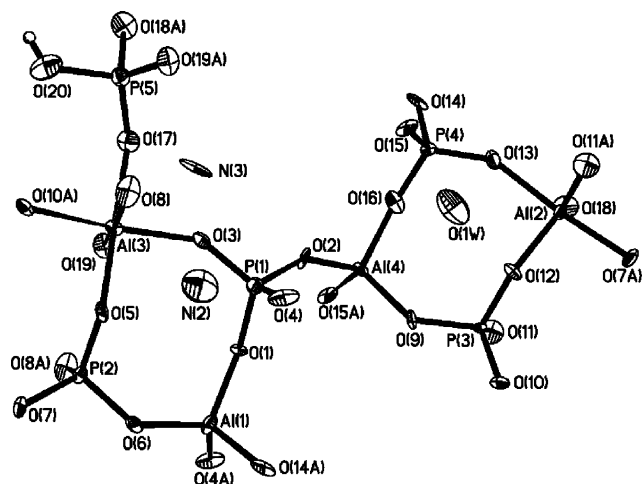


Figure 3. Thermal ellipsoid plot (50%) and atomic labeling scheme of AIPO-CJ19.

AIPO-CJ19 consists of an open framework with macroanion $[\text{Al}_4\text{P}_5\text{O}_{20}\text{H}]^{2-}$. Charge neutrality is achieved by protonated NH_3 molecules. As seen in Figure 3, each asymmetric unit contains four crystallographically distinct Al atoms. Al(1) and Al(4) are tetrahedrally coordinated and share four oxygens with adjacent P atoms with Al–O distances in the range of 1.709(9)–1.785(9) Å. Al(2) is pentacoordinated to five oxygen atoms (Al–O bond lengths: 1.742(7)–1.932(10) Å) to form a distorted trigonal bipyramid. Al(3) is octahedrally coordinated to six oxygen atoms to form a distorted octahedron with Al–O bond lengths in the range of 1.825(8)–1.995(7) Å. To the best of our knowledge, this is the first aluminophosphate in which the Al atoms exist in three kinds of coordination, i.e., AlO_4 , AlO_5 , and AlO_6 , with all of the oxygen atoms connected to P atoms. Of the five crystallographically distinct PO_4 tetrahedra, four (P(1)–P(4)) share all vertex oxygen atoms with adjacent Al atoms. The P–O bond lengths for P(1)–P(4) are in the range of 1.494(8)–1.568(9) Å. P(5) shares only three oxygens with the adjacent Al atoms (2AlO_6 and 1AlO_5) which leaves one oxygen, O(20), terminal. The longer bond length of

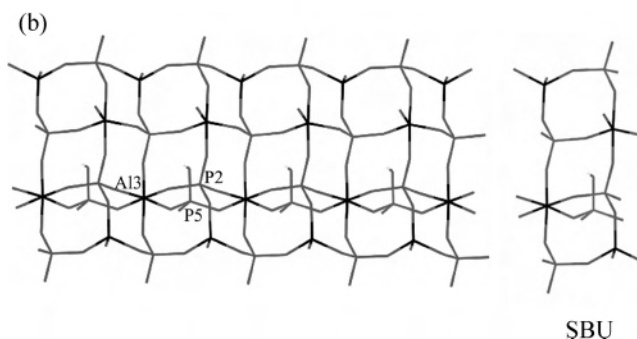
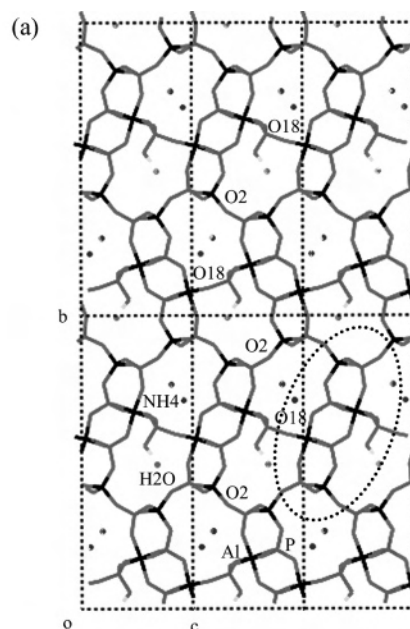


Figure 4. (a) Framework of AIPO-CJ19 viewed along the [100] direction (the dotted frame is shown in (b)). (b) Characteristic network structure in AIPO-CJ19 viewed along [001] direction and the SBU.

1.615(10) Å for P(5)–O(20) indicates a P–OH group which protrudes into the eight-membered ring channels. The existence of P–OH groups in AIPO-CJ19 results in an interrupted open framework with the Al/P ratio deviating from unity, as in the case of JDF-20²³ and AIPO-HDA.¹¹

The open framework of AIPO-CJ19 has eight-membered ring (8-MR) channels along the [100] direction, and the H_2O and protonated NH_3 molecules reside in the channels (Figure 4a). Interestingly, the structure features a series of puckered continuous networks constructed from the ordered connection of Al_2P_2 four-membered rings (4-MR) (Figure 4b). Two types of one-dimensional (1D) aluminophosphate chains, edge-sharing 4-MRs (AIPO-ESC) and corner-sharing 4-MRs (AIPO-CSC), are present in the net and cross-linked at the node of Al(3) and P(2). If P(5) atoms are omitted, the net becomes a square of Al_2P_2 4-MR. The six-coordinated Al(3) atoms are essential for the formation of AIPO-CSC chains. To our knowledge, a network with such an arrangement has never been found in previously reported microporous aluminosilicates and aluminophosphate-based com-

(23) Huo, Q.; Xu, R.; Li, S.; Ma, Z.; Thomas, J. M.; Jones, R. H.; Chippindale, A. M. *J. Chem. Soc., Chem. Commun.* **1992**, 875.

pounds. The secondary building unit (SBU) tool has proven to be helpful for understanding the construction of the framework structures of aluminophosphates and related materials.^{8,24,25} Upon investigation of the open framework of AIPO-CJ19, a new type of SBU, which can be viewed as a branched edge-sharing three 4MR, was found, and the connection of these SBUs results in the network shown in Figure 4b. Adjacent networks are further connected to each other through O(2) and O(18) to compose the 3D open framework. Both AIPO-ESC and AIPO-CSC chains are fundamental building units for the construction of open-framework aluminophosphates.^{26–30} AIPO-ESC or AIPO-CSC chains have been found in some aluminophosphate frameworks, for example, AIPO-CSC chains in JDF-20²³ and AIPO-ESC chains in SAPO-43.³¹ In AIPO-CJ19, both of the chains coexist; this has never before been found in an aluminophosphate family.

The protonated NH₃ molecules, which balance the negative charge of the framework, are trapped in the channels. The H₂O molecules interact with the terminal oxygens attached to P(5) atoms through H-bonds (O(20)–H(1)···O(1W) 2.944(16) Å). The NH₄⁺ cations also form weak hydrogen bonds with the framework oxygen atoms. Each N atom provides two hydrogen bonds to the framework oxygen atoms. The N···O distances are in the range of 2.941–3.088 Å, measured by the Cerius² package.³² Obviously, the NH₄⁺ cations must have come from the fragmentation of 2-aminopyridine under solvothermal conditions. Such a phenomenon has been observed in the previously reported (C₂H₈N)₂[Al₂(HPO₄)(PO₄)₂].³³

Solid-State NMR Spectroscopy. The ²⁷Al MAS NMR spectrum of AIPO-CJ19 acquired at 9.4 T shows four resonances at 44.4, 39.6, ~10, and –14.5 ppm (Figure 5). The two low-field resonances at 44.4 and 39.6 ppm are from the four-coordinated aluminum; the broad one at ~10 ppm is from the five-coordinated aluminum, and the one at –14.5 ppm is from the six-coordinated aluminum. These assignments are based on the approximate chemical shift ranges known to be typical of different aluminum coordinations.^{34,35} The broad line shape of the resonance at ~10 ppm is a result of a second-order quadrupolar interaction which is not

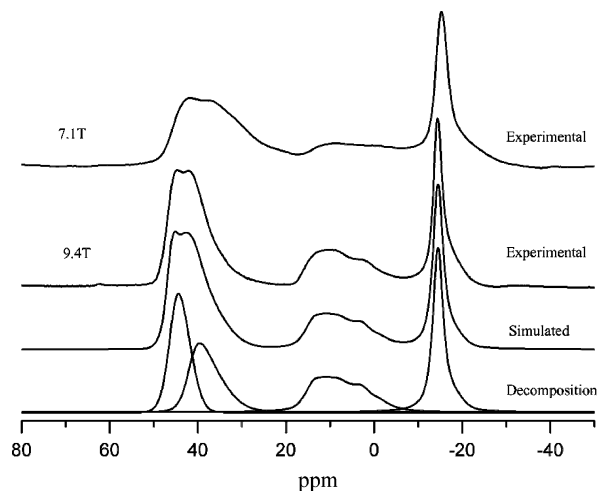


Figure 5. ²⁷Al MAS NMR spectra of AIPO-CJ19 acquired at 9.4 and 7.1 T.

Table 3. ²⁷Al Chemical Shifts and Quadrupolar Interaction Parameters for Different Al Sites in AIPO-CJ19

assignment	$\delta_{\text{exp}}(7.1 \text{ T})$	$\delta_{\text{exp}}(9.4 \text{ T})$	$\Delta\delta_{\text{exp}}$	$\delta_{\text{iso}}(\text{PPM})$	$P_Q(\text{MHz})$	η
Al(1)	33.5	39.6	6.1	47.6	3.8	–
Al(2)	–	–	–	17.0	4.2	0.1
Al(3)	–15.4	–14.5	0.9	–13.4	1.4	–
Al(4)	41.5	44.4	2.9	48.1	2.6	–

completely removed by MAS. To obtain the parameter of quadrupolar interaction (P_Q) and the isotropic chemical shift (δ_{iso}) for four- and six-coordinated aluminum atoms, a ²⁷Al MAS NMR experiment was carried out at a different field of 7.1 T.^{36,37} The line width (Figure 5) becomes broader and the high-field shift appears because of the increase of the second-order quadrupolar interaction in a relatively low field. On the basis of the difference between the chemical shift values at two different fields, it is easy to obtain P_Q and δ_{iso} with eqs 1 and 2

$$\Delta\delta_{\text{exp}} = 6 \times 10^3 P_Q^2 \left[(1/\nu_0')^2 - (1/\nu_0'')^2 \right] \quad (1)$$

$$\delta_{\text{iso}} = \delta_{\text{exp}} + 6 \times 10^3 \left(\frac{P_Q}{\nu_0} \right)^2 \quad (2)$$

where ν_0 is the resonance frequency of ²⁷Al in different fields. The detailed experimental results are listed in Table 3. The simulations of the ²⁷Al MAS spectrum were performed using the DMFIT program,³⁸ and the P_Q , δ_{iso} , and asymmetry parameter (η_Q) for the five-coordinated aluminum atoms are obtained and listed in Table 3. The simulated spectrum and its decomposition indicate that the corresponding four-, five-, and six-coordinated aluminum atoms are present in a ratio of 2/1/1 which is consistent with the structure determined by the single-crystal XRD analysis. It has been demonstrated

- (24) Yu, J.; Sugiyama, K.; Hiraga, K.; Togashi, N.; Terasaki, O.; Tanaka, Y.; Nakata, S.; Qiu, S.; Xu, R. *Chem. Mater.* **1998**, *10*, 3636.
 (25) Férey, G. *Chem. Mater.* **2001**, *13*, 3084.
 (26) Jones, R. H.; Thomas, J. M.; Xu, R.; Huo, Q.; Xu, Y.; Cheetham, A. K.; Bieber, D. *J. Chem. Soc., Chem. Commun.* **1990**, 1170.
 (27) Williams, I. D.; Yu, J.; Gao, Q.; Chen, J.; Xu, R. *Chem. Commun.* **1997**, 1273.
 (28) Wei, B.; Yu, J.; Shi, Z.; Qiu, S.; Yan, W.; Terasaki, O. *Chem. Mater.* **2000**, *12*, 2065.
 (29) Wang, K.; Yu, J.; Song, Y.; Xu, R. *J. Chem. Soc., Dalton Trans.* **2003**, 99.
 (30) Wang, K.; Yu, J.; Li, C.; Xu, R. *Inorg. Chem.* **2003**, *42*, 4597.
 (31) Helliwell, M.; Kaucic, V.; Cheetham, G. M. T.; Harding, M. M.; Kariuki, B. M.; Rizkallah, P. *J. Acta Crystallogr., Sect. B* **1993**, *49*, 413.
 (32) *Cerius 2*; Molecular Simulations/Biosym Corporation: San Diego, CA, 1995.
 (33) Song, Y.; Yu, J.; Li, Y.; Li, G.; Xu, R. *Angew. Chem., Int. Ed.* **2004**, *43*, 2399.
 (34) Zahedi-Niaki, M. H.; Xu, G.; Meyer, H.; Fyfe, C. A.; Kaliaguine, S. *Microporous Mesoporous Mater.* **1999**, *32*, 241.
 (35) Blackwell, C. S.; Patton, R. L. *J. Phys. Chem.* **1984**, *88*, 6135.

- (36) Massiot, D.; Müller, D.; Hübert, Th.; Schneider, M.; Kentgens, A. P. M.; Coté, B.; Coutures, J. P.; Gessner, W. *Solid State Nucl. Magn. Reson.* **1995**, *5*, 175.
 (37) Azaïs, T.; Bonhomme-Courry, L.; Vaissermann, J.; Bertani, P.; Hirschinger, J.; Maquet, J.; Bonhomme, C. *Inorg. Chem.* **2002**, *41*, 981.
 (38) Massiot, D.; Fayon, F.; Capron, M.; King, I.; Le Calvé, S.; Alonso, B.; Durand, J.-O.; Bujoli, B.; Gan, Z.; Hoatson, G. *Magn. Reson. Chem.* **2002**, *40*, 70.

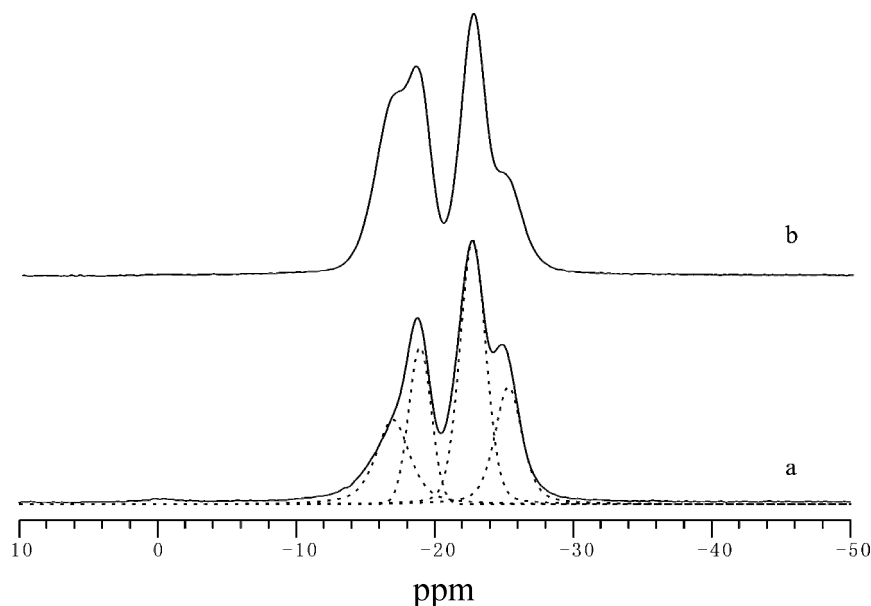


Figure 6. (a) ^{31}P MAS NMR spectrum and (b) $^1\text{H} \rightarrow ^{31}\text{P}$ CPMAS NMR spectrum of AIPO-CJ19 (the dashed lines indicate the decomposition of the ^{31}P spectrum).

that a more distorted tetrahedral site will have a stronger quadrupolar interaction.³⁹ A parameter ψ was proposed as a measurement of the distortion (eq 3)

$$\Psi = \sum_i \tan|\theta_i - 109.5^\circ| \quad (3)$$

where θ_i is the i th O–Al–O bond angle and is equal to 109.5° for perfect tetrahedral symmetry. On the basis of the O–Al–O bond angles determined for AIPO-CJ19 by single-crystal XRD analysis, eq 3 yields $\psi_{\text{Al}(1)} = 0.248$ and $\psi_{\text{Al}(4)} = 0.169$. Thus, the signal corresponding to $P_Q = 3.8$ is assigned as Al(1), and the other signal corresponding to $P_Q = 2.6$ is assigned as Al(4).

The ^{31}P MAS NMR spectrum of AIPO-CJ19 in Figure 6a shows four components located at -16.7 , -18.8 , -22.7 , and -25.2 ppm. The deconvolution of the spectrum with Gaussian lines (dashed line in Figure 6a) indicates that the integrated intensity ratio of the four resonances is close to $1/1/2/1$, suggesting the presence of five distinct crystallographic phosphorus sites, in good agreement with the structure determined by the single-crystal XRD. The shift at -16.7 ppm is a result of the P(5) tetrahedron with a terminal oxygen belonging to a hydroxyl group for its smaller shielding effect, which has been proven by the $^1\text{H} \rightarrow ^{31}\text{P}$ CPMAS technique. In the $^1\text{H} \rightarrow ^{31}\text{P}$ CPMAS NMR spectrum (Figure 6b) with a contact time of 0.2 ms, the intensity of the resonance at -16.7 ppm is increased significantly which confirms the assignment of that resonance to P(5). P(1)–P(4) lie within the characteristic chemical shift range of $\text{P}(\text{OAl})_4$ species.^{40,41} The two phosphorus sites, corresponding to the component at -22.7 ppm, are probably in a

Table 4. Environments and Chemical Shifts for Different P Sites

	environment of P			chemical shift (PPM)
P(1)	1AlO ₆		3AlO ₄	−22.7
P(2)	2AlO ₆	1AlO ₅	1AlO ₄	−25.2
P(3)	1AlO ₆	2AlO ₅	1AlO ₄	−22.7
P(4)		AlO ₅	3AlO ₄	−18.8
P(5)	2AlO ₆	AlO ₅		−16.7

very similar environment. It has been shown that the presence of Al atoms with coordination states higher than four in aluminophosphates may result in a decrease of ^{31}P chemical shifts.⁴² Therefore, in AIPO-CJ19, the number of five- and six-coordinated Al neighbors must be taken into consideration. The environments of different P sites are listed in Table 4. As can be seen in Table 4, P(2) has the highest number of six- and five-coordinated Al neighbors. Therefore P(2) is tentatively assigned to the chemical shift at -25.2 ppm. Accordingly, P(1) and P(3) may contribute to the component at -22.7 ppm, and P(4) may contribute to the component at -18.8 ppm.

Various Coordinations of Al and P of Aluminophosphates with an Al/P Ratio of 4/5. Until now, four unique structural connectivities with an Al/P ratio of 4/5 have been known, including the 2D layer Mu-4¹² and the 3D open-framework AIPO-HDA,¹¹ SIZ-1,¹³ and AIPO-CJ19. Mu-4 and SIZ-1 are based on the alternation of 3AlO_4 , 1AlO_5 , 3PO_{4b} , $1\text{PO}_{3b}\text{O}_t$, and $1\text{PO}_{2b}\text{O}_{2t}$; AIPO-HDA is based on the alternation of 2AlO_4 , 2AlO_5 , 4PO_{4b} , and $1\text{PO}_{2b}\text{O}_{2t}$, and AIPO-CJ19 is based on the alternation of 2AlO_4 , 1AlO_5 , 1AlO_6 , 4PO_{4b} , and $1\text{PO}_{3b}\text{O}_t$. We have found the relationship between the Al/P ratio and the Al and P coordination states⁸ which satisfies eq 4

$$\sum_i m_{\text{AlO}ib} \times i_{\text{AlO}ib} = \sum_j n_{\text{PO}jb} \times j_{\text{PO}jb} \quad (4)$$

where i (j) is the number of bridging oxygens coordinated

(39) Engelhardt, G.; Veeman, W. *J. Chem. Soc., Chem. Commun.* **1993**, 622.

(40) Caldarelli, S.; Meden, A.; Tuel, A. *J. Phys. Chem. B* **1999**, *103*, 5477.

(41) Jelinek, R.; Chmelka, B. F.; Wu, Y.; Grandinetti, P. J.; Pines, A.; Barrie, P. J.; Klinowski, J. *J. Am. Chem. Soc.* **1991**, *113*, 4097.

(42) Akporiaye, D. E.; Stöcker, M. *Zeolites* **1992**, *12*, 351.

Table 5. All Possible Coordinations of Al and P of the Aluminophosphates with an Al/P Ratio of 4/5

no	Al coordination			P coordination			ref ^a	
	AlO ₄	AlO ₅	AlO ₆	PO _{4b}	PO _{3b} O _t	PO _{2b} O _{2t}		PO _b O _{3t}
1	4	0	0	3	1	0	1	—
2	4	0	0	3	0	2	0	—
3	4	0	0	2	2	1	0	—
4	4	0	0	1	4	0	0	—
5	3	1	0	4	0	0	1	—
6	3	1	0	3	1	1	0	Mu-4, SIZ-1
7	3	1	0	2	3	0	0	—
8	3	0	1	4	0	0	1	—
9	3	0	1	3	2	0	0	—
10	2	2	0	4	0	1	0	AIPO-HDA
11	2	2	0	3	2	0	0	—
12	2	1	1	4	1	0	0	AIPO-CJ19
13	2	0	2	5	0	0	0	—
14	1	3	0	4	1	0	0	—
15	1	2	1	5	0	0	0	—
16	0	4	0	5	0	0	0	—

^a The — means not found.

to Al(P), $m(n)$ is the number of the AlO_{*i*} (PO_{*j*}) coordination, $m_{\text{AlO}_i}/n_{\text{PO}_j} = \text{Al/P}$, $i = 3, 4, 5$, and 6, corresponding to the AlO₃(OH), AlO₄, AlO₅, and AlO₆ coordinations, respectively, and $j = 1, 2, 3$, and 4, corresponding to PO₄ tetrahedra with one, two, three, and four bridging oxygens, respectively.

On the basis of eq 4, all possible coordinations of the Al and P atoms of the aluminophosphates with an Al/P ratio of 4/5 are calculated and listed in Table 4. Sixteen combinations of different Al and P coordinations may lead to the [Al₄P₅O₂₀]³⁻ stoichiometry. Among them, the three known combinations with four unique structural connectivities are indicated in bold in Table 5.

It is well-known that solid-state NMR techniques are sensitive to local orderings and geometries. They will be helpful for distinguishing different Al and P coordinations and will serve as a useful tool for the understanding of aluminophosphate structures.

Conclusions

AIPO-CJ19, with an Al/P ratio of 4/5, has been synthesized solvothermally in the Al(OPr^{*i*})₃-H₃PO₄-2-aminopyridine-pyridine system. It is composed of strictly alternating Al units, including AlO₄, AlO₅, and AlO₆, and P tetrahedra, including PO_{4b} and PO_{3b}OH, to form a 3D open framework with 8-MR channels along the [100] direction. Solid-state NMR techniques confirm the single-crystal X-ray diffraction analysis results. The ²⁷Al MAS NMR spectrum indicates four Al signals with a ratio of 2AlO₄/1AlO₅/1AlO₆. The ³¹P MAS NMR spectrum presents five tetrahedral P signals with a ratio of 1/1/2/1. Sixteen combinations of Al and P coordinations, which may lead to the [Al₄P₅O₂₀]³⁻ stoichiometry, are summarized. Until now, three combinations have been known. It is believed that many more new aluminophosphates with [Al₄P₅O₂₀]³⁻ stoichiometry will be continuously synthesized.

Acknowledgment. This work is supported by the National Natural Science Foundation of China and the State Basic Research Project of China (G2000077507).

Supporting Information Available: Crystallographic data (CIF), atomic coordinates with isotropic temperature factors, and selected bond lengths and angles for AIPO-CJ19 (pdf). This material is available free of charge via the Internet at <http://pubs.acs.org>.

IC048476X